The 19th Conference of Mechanical Engineering Network of Thailand
19-21 October 2005, Phuket, Thailand

# Design of the New 4-DOF Parallel Manipulator with Object Contact Force Control

Viboon Sangveraphunsiri and Natdanai Tantawiroon
Robotics and Advanced Manufacturing Lab Department of Mechanical Engineering
Chulalongkorn University
254 Phyathai Patumwan Bangkok 10330 Thailand
Tel. 66-2218-6448, 66-2218-6585 Fax 66-2218-6583
E-mail Viboon.S@eng.chula.ac.th, reverserp@eng.chula.ac.th

## Abstract
This paper presents novel design of the parallel manipulator of the H-4 family parallel robot with three degrees of freedom (DOF) in translation and one in rotation. Thorough analysis of forward and inverse position and velocity relationships are presented. Further more, when tackled with turn table forming 5th axis, this design can perform nearly all the tasks such as milling and rapid prototyping. Author use inverse stiffness matrix (Compliance matrix) to calculate the direction of “deflection” of robot in task space, in conjunction with arm stiffness, the controller command the arm to move “into” the object thus produce force. The proposed force control scheme show good tracking response in various testing conditions; the force fluctuation is within ±5-newton range with 30 percent overshoot. The future work concentrate on human-machine interface in the rapid prototyping task for more accurate and complicate path planning and better surface finishing.

**Keywords**: Parallel, Manipulator, Kinematics

## 1. Introduction

The parallel robot is one of the subjects that the communities have paid great contribution for the past several years. Since Gouge and Stewart [1] proposed the earliest form of practical parallel manipulator for testing and simulation purpose, the research in parallel robot continued to grow. The parallel robot configuration performs variety of task ranged from simple pick-and-place to complex machining. The advantages of parallel manipulator over serial manipulator are high load capacity, higher stiffness and lower link inertia, while to the contrary, serial-link robot excel in large workspace and offer more flexibility. Due to these characteristics, parallel robots are perfect for milling or coordinate measuring machines, thanks to their large capacity and rigidity. The shortcomings of parallel robot are generally kinematics difficulties, small workspace and mobility (workspace of robot when the moving platform is tilting is usually smaller) compare to its serial counterpart. From overall criteria analysis, new design has been proposed by authors in [2]. Contrary to general Stewart-platform type machine or one would call “Hexapod” for its six-leg configuration; the new parallel arm contains four DOF via its quad actuators and leg mechanism. The design has simpler kinematics expression and, in fact, if coupled with turn table forming the 5th axis, should be enough for overall application. The design consideration and detailed kinematics analysis has also been review in [2] and will briefly be discuss in the following sections, including Forward and Inverse kinematics.

For background of parallel kinematics and theory, reader should consult with [1]. The general form of parallel machine varies from three to six DOF are detailed in [3-6]. Especially, the 4 DOF design, namely “H-4” has been proved and reviewed in [7-8]. The 5-DOF is shown in [9]. Although lesser-than-sixth DOF robot has less complex kinematics but in general, forward kinematics solution still can not be expressed in closed form as shown in [7] which states that the forward kinematics solutions are in the form of $8^{th}$ order polynomial.

The developed arm aimed at performing man-machine task, has been tested for the abilities of force tracking control on unknown object surface. In application such as automated CMM machine, Rapid Prototyping with man-machine interface, force tracking is vital to maintain robot accuracy and also safety working condition. Various force control scheme has been proposed, early effective force-position hybrid control proposed by [10-12]. Also force impedance control by [13]. The algorithm in question must be robust and adaptive to effectively follow the surface without prior knowledge of object geometry. [12-13], present more robust control scheme which adjust stiffness in account for uncertainty of both robot and environment. More adaptive and intelligence control technique such as Neuro-Fuzzy method was used in [14-17]. Additionally, auto parts assembly using force guided parallel robot is introduced in [18]. Due to the robot configuration, inverse of stiffness matrix, compliance matrix has been obtained in analytical form. This compliance matrix is position dependent and calculated arm deflection is also force direction dependent. Of which, combine with knowledge of actual interaction force between robot tool tip and object measured by mean of force transducer, one can calculate resultant deflection of robot depending on robot position and actual force measurement which lead to position command fetch to arm controller result in more robust tracking behavior. The prototype performed force tracking task on an unknown object surface utilizing the stiffness and compliance matrix obtained priory from kinematics analysis.

## 2. Proposed Design

From above discussion, the author presents H-4 family parallel mechanism as shown in figure 1a and 1b. Machine consists of four actuators which are $\mathbf{l_1}$ $\mathbf{l_2}$ $\mathbf{l_3}$ and $\mathbf{l_4}$ all point to x direction of machine coordinate. Four legs AB of length R comprise of PUU joints connected to the moving platform via two revolute joints at C result in rotation in y.

Designing parameters are leg length R and the difference between platform size and footprint (a-b). Parameters determination depends on number of factors result in optimization of mechanism characteristics such working volume. In order to determine robot working boundary, forward position relationship which transfer allowable input actuators length into corresponded motion boundary must first be carryout.

### 2.1 Inverse Kinematics

In order to keep the paper organized, some robot core concept has been review here. Consider robot schematic diagram shown in figure 1a) and 1b), let P = {x, y, z, θ} be the robot position and $\{l_1, l_2, l_3, l_4\}$ be the robot input actuators length, so

$$l_1 = x_1 \pm \sqrt{R^2 - {y_1}^2 - {z_1}^2}$$

But consider the geometric configuration of robot there is only one solution which is,

$$l_1 = x_1 + \sqrt{R^2 - {y_1}^2 - {z_1}^2} \qquad (1)$$

Where $x_1$ is the position of point $\mathbf{B_{1,\,2}}$ at the triangle formed by leg $\mathbf{A_1B_1}$ and $\mathbf{A_2B_2}$ as shown in figure 1a) and 1b) and found to be,

$$\begin{aligned} x_1 &= x + c\cdot\sin(\theta) \\ y_1 &= y + b - a \\ z_1 &= z + c\cdot\cos(\theta) - d \end{aligned}$$

In the same pattern,

$$l_2 = x_1 - \sqrt{R^2 - {y_1}^2 - {z_1}^2} \qquad (2)$$

For actuator 3 and 4 found that,

$$\begin{aligned} l_3 &= x_2 + \sqrt{R^2 - {y_2}^2 - {z_2}^2} \\ l_4 &= x_2 - \sqrt{R^2 - {y_2}^2 - {z_2}^2} \end{aligned} \qquad (3), (4)$$

Where $x_2$ is also the position of point $\mathbf{B_{3,\,4}}$ as shown in figure 1a) and 1b) and found to be,

$$\begin{aligned} x_2 &= x - c\cdot\sin(\theta) \\ y_2 &= y - b + a \\ z_2 &= z - c\cdot\cos(\theta) + d \end{aligned}$$

Equations (1) to (4) are used to solve for corresponded actuators length for the given platform position.

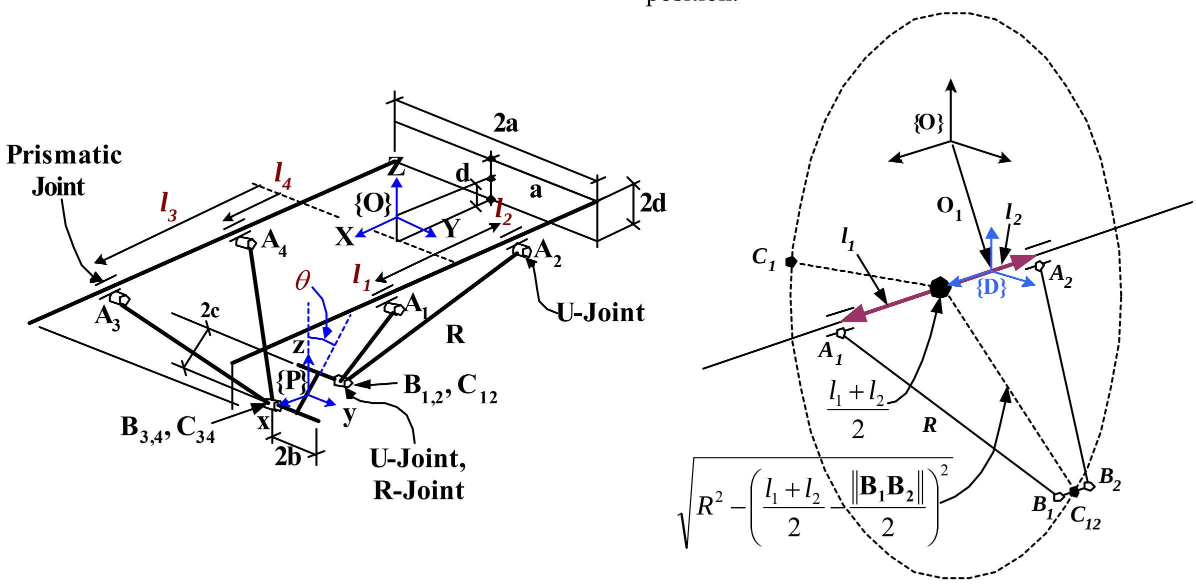


**Figure 1** Proposed 4 DOF arm a) Robot joint configuration and b) Moving path of point B

### 2.2 Forward kinematics analysis

From robot input parameter $\mathbf{l_1}$ $\mathbf{l_2}$ $\mathbf{l_3}$ and $\mathbf{l_4}$, we assume new variable depended on these inputs to be,

$$r_1 = \frac{l_1 + l_2}{2}, r_2 = \frac{l_3 + l_4}{2}, d_1 = l_1 - l_2, d_2 = l_3 - l_4$$

Which can be described as: $r_1$ and $r_2$ are position of the plane containing path of point B, $d_1$ and $d_2$ are radius of circle form by trajectory of point B as in figure 1b). As one already seen from above description, difference between $r_1$ and $r_2$ in conjunction with platform parameter c which is the distance between $\mathbf{B_{1,\,2}}$ and $\mathbf{B_{3,\,4}}$ results in the rotation of platform in y axis.

Rotation of platform can readily be determined as

$$\cos(\theta)=\frac{\sqrt{4c^2-(r_1-r_2)^2}}{2c} \tag{5}$$

As well as the rotation, the movement in x direction is easily obtain

$$x=\frac{r_1+r_2}{2} \tag{6}$$

We can independently acquire two of four forward kinematics solutions. As for motion in y and z, manipulating equations (1) to (4) yield y in the form of z in two independent equations as shown below.

$$y=\frac{d_1^2-d_2^2+8z\left[\sqrt{4c^2-(r_2-r_1)^2}-2d\right]}{16(a-b)} \tag{7}$$

$$\frac{d_1{}^2+d_2{}^2}{4}=2R^2-2y^2-2(b-a)^2-2z^2 -2(c\cdot\cos(\theta)-d)^2 \tag{8}$$

Substitute equation (8) into y in (7) result in 2nd order polynomial of z which can be solved using simple formula

$$z=\frac{-B\pm\sqrt{B^2-4AC}}{2A}$$

Due to the configuration of robot proposed, the solution in z is always negative, of which, the coefficients A, B and C were found to be

$$A=\frac{\left[\sqrt{4c^2-(r_2-r_1)^2}-2d\right]^2}{2(a-b)^2}+2$$

$$B=\frac{\left(d_1^2-d_2^2\right)\left[\sqrt{4c^2-(r_2-r_1)^2}-2d\right]}{8(a-b)^2}$$

$$C=\frac{d_1{}^2+d_2{}^2}{4}-2R^2+2(b-a)^2+ \frac{1}{2}\left[\sqrt{4c^2-(r_2-r_1)^2}-2d\right]^2+\frac{\left(d_1{}^2-d_2{}^2\right)^2}{128(a-b)^2} \tag{9}$$

## 3. Force Control Implementation

The purpose of this article is to propose the control scheme using nearly accurate knowledge of robot characteristics represent by forward kinematics and Jacobian matrix to help improve the efficiency of force tracking control. The general method for hybrid force-position control by tracking and adjust object virtual stiffness instead of directly track the force itself is called implicit force control contrary to explicit control. This can be describing as controlling force by controlling distance which resulted from force instead. By estimated the stiffness of environment and calculate required distance for the manipulator to move “into” the object thus produce force. The uncertainty of robot model and environment geometry and stiffness can be corrected by means of integral term with some significant gain.

In order to calculate tracking direction, one utilizes this simple vector relation as shown in figure 2 and the force control scheme was implemented as shown in figure 3.

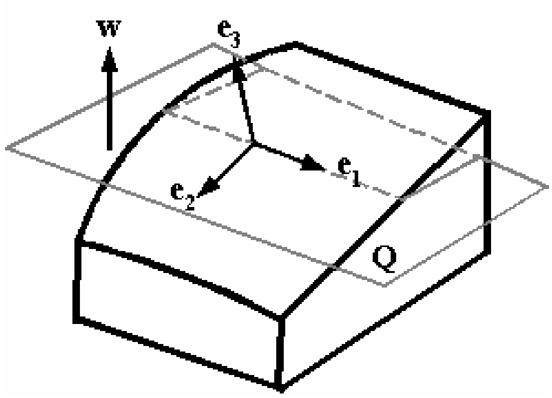


**Figure 2** Determining Tracking direction in desired tracking plane from measured force

### 3.1 Stiffness Matrix

If computed stiffness is close to the actual stiffness, the position command should settle quickly thus more stability. From [19] stiffness matrix of parallel manipulator is found to be,

$$\mathbf{F}=\mathbf{J}^{\mathrm{T}}\mathbf{kJ\delta} \tag{10}$$

Where the configuration dependent stiffness matrix, F is force vector applied at robot end position, is corresponded displacement at robot’s end and k is the diagonal matrix whose elements are actuator stiffness. As seen, stiffness is position dependent and the displacement is also depended on force vector whose direction is not necessarily the same.

### 3.2 Compliance Matrix

In case of force vector is known from transducer, the displacement is obtained by inverse the stiffness matrix, which is known as compliance matrix,

$$\mathbf{\Lambda F}=\boldsymbol{\delta} \tag{11}$$

Where,

$$\mathbf{\Lambda}=\begin{bmatrix} a_{11} & a_{12} & \cdots & a_{1n} \\ a_{21} & \ddots & & a_{2n} \\ \vdots & & \ddots & \vdots \\ a_{n1} & a_{n2} & \cdots & a_{nn} \end{bmatrix}$$

Each elements of compliance matrix can be found by calculate resulted motion of each joint due to applied unit force in each DOF. Thus, $a_{ij}$ is the displacement of joint i due to applied unit force in DOF j. In case of all actuators have identical stiffness k; the compliance matrix for manipulator can be obtained using free-body diagram approach as seen in figure 4a. The manipulator has three DOF in translation and one in rotation so in case where unit force applied in x direction, assuming all legs is two-force member; the force acting on each actuator is only the x component of force in leg link. The force must satisfied equilibrium conditions,

$$\sum F_x = 0, \sum F_y = 0, \sum F_z = 0 \text{ and } \sum M_y = 0$$

Noting that these static conditions do not applied for equilibrium of moment in x and z axis assuming the metachain in each side of mechanism can produced internal moment to neutralize the resultant moments in x and z.

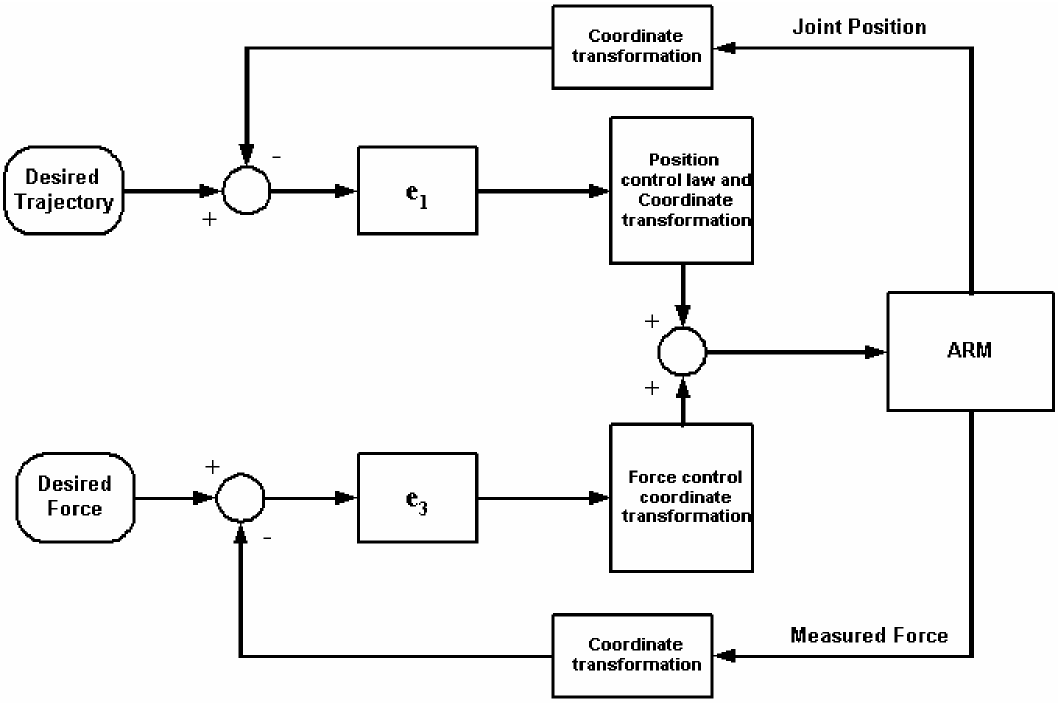


**Figure 3** Implicit force control scheme used on prototype manipulator

From above method, all elements of compliance matrix, by using the angle notation α and β as shown in figure 4, were found to be,

In case where unit force applied in x direction,

$$\tau_{11} = \tau_{12} = \tau_{13} = \tau_{14} = \frac{1}{4} \quad (12)$$

In case where unit force applied in y direction,

$$\tau_{21} = \frac{\sin\beta_2}{2\sin(\beta_1+\beta_2)\cdot\tan\alpha_1} + \frac{\sin\beta_1\cdot\sin\beta_2}{2\sin(\beta_1+\beta_2)}\tan\theta$$

$$\tau_{22} = -\frac{\sin\beta_2}{2\sin(\beta_1+\beta_2)\cdot\tan\alpha_1} + \frac{\sin\beta_1\cdot\sin\beta_2}{2\sin(\beta_1+\beta_2)}\tan\theta$$

$$\tau_{23} = -\frac{\sin\beta_1}{2\sin(\beta_1+\beta_2)\cdot\tan\alpha_2} - \frac{\sin\beta_1\cdot\sin\beta_2}{2\sin(\beta_1+\beta_2)}\tan\theta$$

$$\tau_{24} = \frac{\sin\beta_1}{2\sin(\beta_1+\beta_2)\cdot\tan\alpha_2} - \frac{\sin\beta_1\cdot\sin\beta_2}{2\sin(\beta_1+\beta_2)}\tan\theta$$

(13)

In case where unit force applied in z direction,

$$\tau_{31} = \frac{\cos\beta_2}{2\sin(\beta_1+\beta_2)\cdot\tan\alpha_1} + \frac{\sin(\beta_1-\beta_2)}{4\sin(\beta_1+\beta_2)}\tan\theta$$

$$\tau_{32} = -\frac{\cos\beta_2}{2\sin(\beta_1+\beta_2)\cdot\tan\alpha_1} + \frac{\sin(\beta_1-\beta_2)}{4\sin(\beta_1+\beta_2)}\tan\theta$$

$$\tau_{33} = \frac{\cos\beta_1}{2\sin(\beta_1+\beta_2)\cdot\tan\alpha_2} - \frac{\sin(\beta_1-\beta_2)}{4\sin(\beta_1+\beta_2)}\tan\theta$$

$$\tau_{34} = -\frac{\cos\beta_1}{2\sin(\beta_1+\beta_2)\cdot\tan\alpha_2} - \frac{\sin(\beta_1-\beta_2)}{4\sin(\beta_1+\beta_2)}\tan\theta$$

(14)

As for the moment equation case,

$$\tau_{41} = \tau_{42} = -\frac{1}{4c\cdot\cos\theta}$$

And

$$\tau_{43} = \tau_{44} = \frac{1}{4c \cdot \cos\theta} \qquad (15)$$

Hence compliance matrix is in the form,

$$\mathbf{\Lambda}(\mathbf{x}) = \mathbf{J}^{-1}\mathbf{k}^{-1}\left(\mathbf{J}^{\mathbf{T}}\right)^{-1}$$

$$= \frac{1}{k}\begin{bmatrix} \tau_{11} & \tau_{12} & \tau_{13} & \tau_{14} \\ \tau_{21} & \tau_{22} & \tau_{23} & \tau_{24} \\ \tau_{31} & \tau_{32} & \tau_{33} & \tau_{34} \\ \tau_{41} & \tau_{42} & \tau_{43} & \tau_{44} \end{bmatrix} \bullet \begin{bmatrix} \tau_{11} & \tau_{21} & \tau_{31} & \tau_{41} \\ \tau_{12} & \tau_{22} & \tau_{32} & \tau_{42} \\ \tau_{13} & \tau_{23} & \tau_{33} & \tau_{43} \\ \tau_{14} & \tau_{24} & \tau_{34} & \tau_{44} \end{bmatrix} \qquad (16)$$

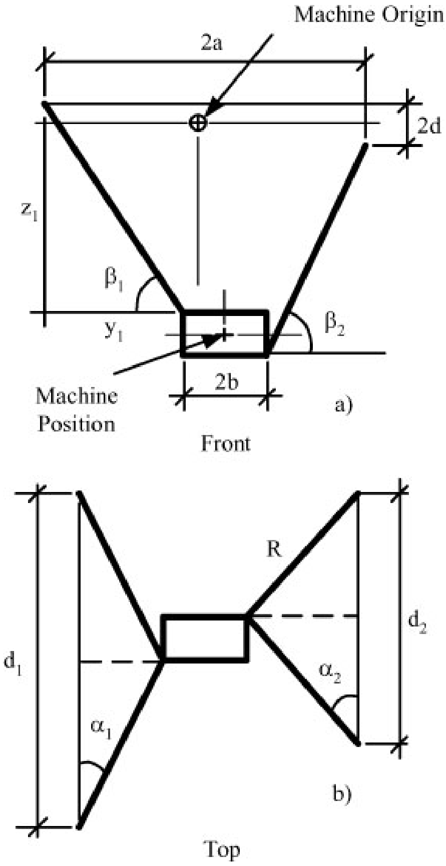


**Figure 4** Position of manipulator viewing from the front and top represented by angle $\alpha_1$ $\alpha_2$ $\beta_1$ and $\beta_2$

## 4. Experimental Results

The controller used in the robot arm is dSpace 1103 operate at 50 µs for servo loop and 1 ms for command loop. New position command from force control loop is also update at 1 ms interval. Force measurement use ATI six axis mini45 Force transducer. Sensor read-out through A/D converter is filtered using soft-digital low-pass filter. The prototype robot is shown in figure 5. Figure 5a) show the all-parallel actuators and figure 5b) detailed the moving platform revolute joints and force sensor. The robot has the following parameters (please refer to figure 1), length of legs is 400mm, size of robot (a-b) is 143 mm and platform size c and d are both 20mm.

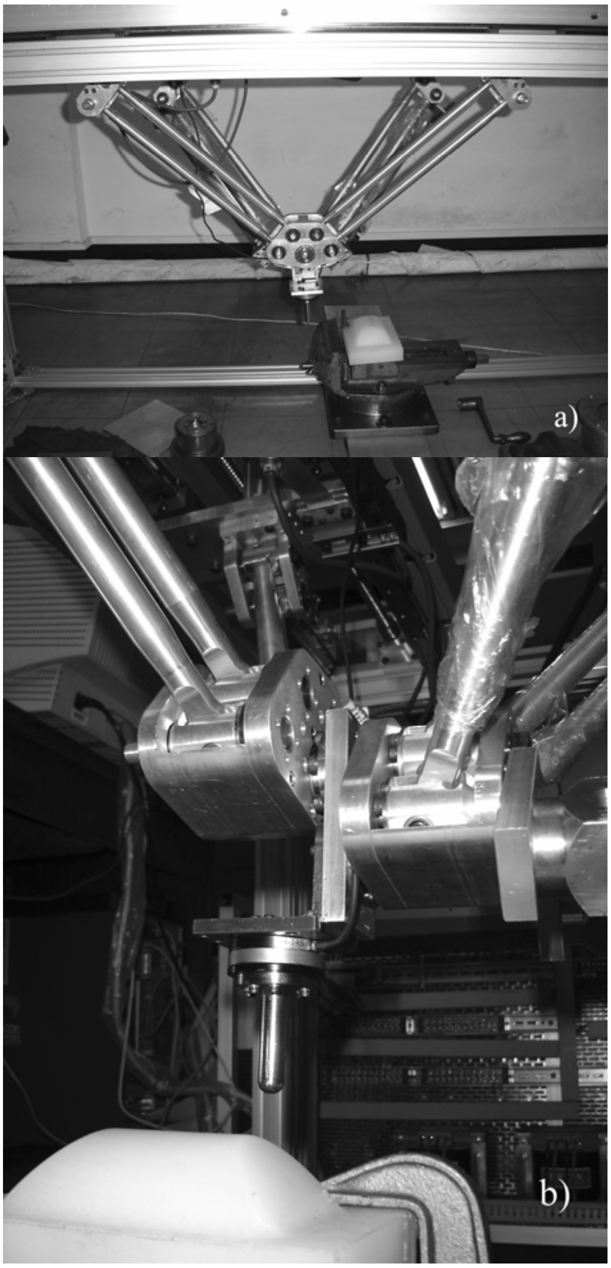


**Figure 5** a) Prototyped new H-4 family parallel manipulator and b) Detail of moving platform and ATI mini45 force transducer of the prototyped new H4 family Manipulator

Force tracking control on resin in direction shown in figure 6a at 20 and 30 N using track speed of 15 and 30 cm/min result is shown in figure 6b) and 6c). Also experiment with step input change from 30 to 15 N is shown in figure 6d). Better result is achieved when tracking large force especially in z axis, due to the high stiffness in z, the response oscillating more when there is more force component in z. The average force tracking accuracy is within the range of 5 N and overshoot is around 30%-50%.

Force tracking control on metal surface in tracking direction as shown in figure 7a) is shown in figure 7b) and 7c). Also, tracking result on aluminum surface in the same configuration as figure 7a) using tracking speed of 60 cm/min. is shown in figure 7d.The result shows similar trend of response. Tracking response for large force is better than small force. The error is also within range of 5 N with no overshoot.

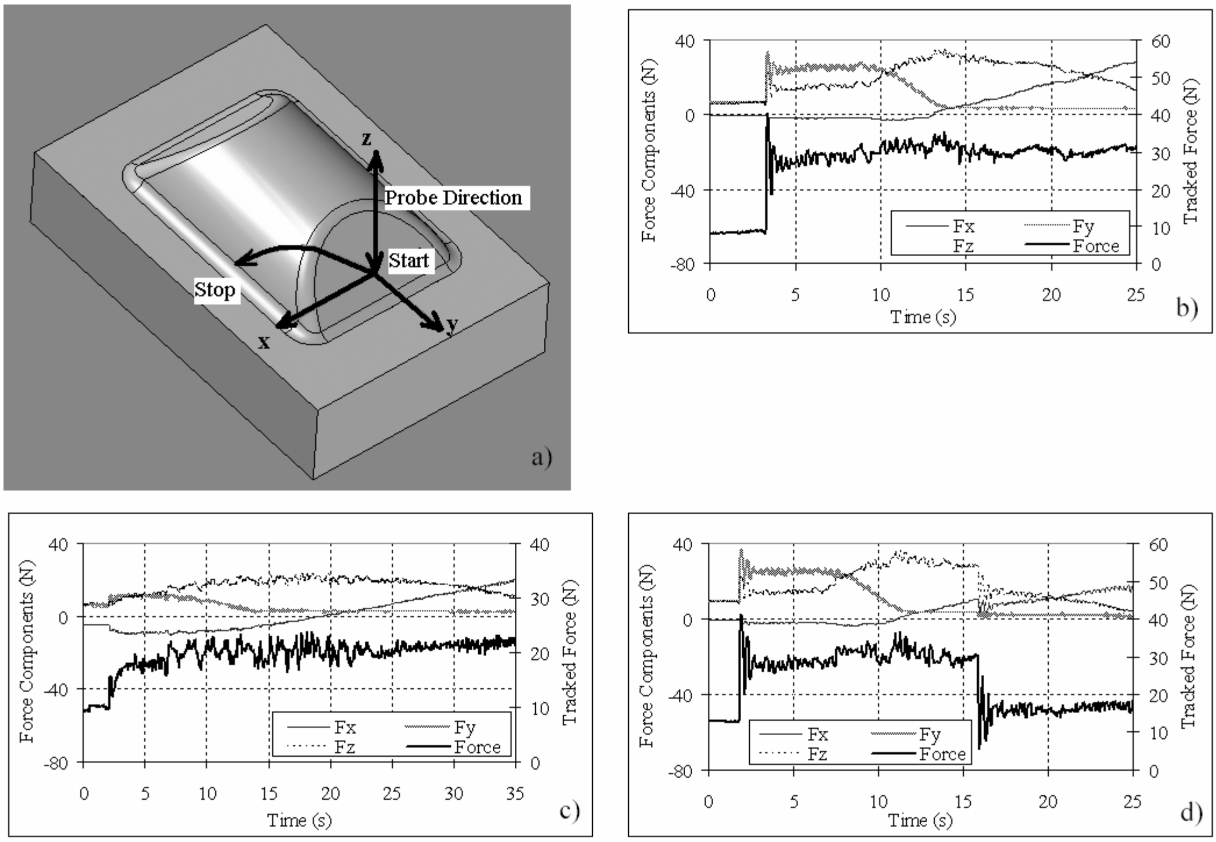


**Figure 6** a) Force tracking direction on resin surface b) Force tracking control on resin at 30 N and track speed at 21 cm/min. c) Force tracking control on resin at 20 N and track speed at 15 cm/min. and d) Force tracking control on resin with force step input changed from 30 to 15 N and tracking speed of 21 cm/min

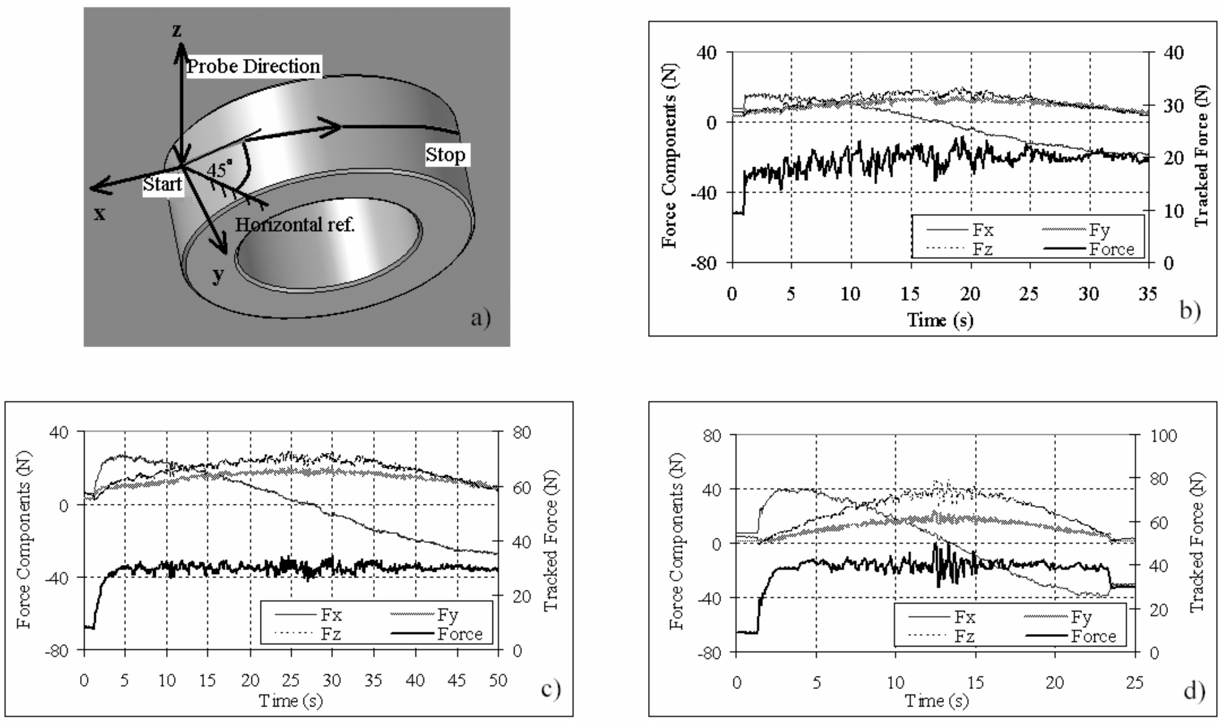


**Figure 7** a) Tracking direction on metallic surface b) Force tracking control on metal at 20 N and track speed at 21 cm/min c) Force tracking control on metal at 30 N and track speed at 21 cm/min and d) Force tracking control on Aluminum at 40 N and track speed at 60 cm/min

## 5. Conclusions

In this paper, extensive analysis of the new H-4 family parallel manipulator has been presented. The inverse kinematics and especially forward kinematics can be represented in closed form. Implicit hybrid force-position control scheme has been implemented using robot compliance to compute the corresponded deflection due to compression in arbitrary position. The results show good characteristics and controllability. In the future, researched should be realized in dynamic modeling of the manipulator for more precise arm control, also actual stiffness of robot arm which depends on both configuration and construction should be accounted for. At present, the other parallel master arm will be incorporated to create the force and position haptic display for human-assist rapid prototyping machine aimed for more precise and efficient cutting path generation and better finished product.

## Acknowledgement

The author wishes to thanks Chulalongkorn University for supporting the research under the HM 72nd anniversary research assisting fund.

## References

[1] Stewart, D. (1965) A platform with 6 degrees of freedom. Proc. Institution of mechanical engineers, 180 (part 1, 15): 371-386.
[2] Sangveraphunsiri, V., Tantawiroon, N. (2003) Novel Design of a 4DOF Parallel Robot. Proc. JSAE Annual Congress, No.61-03: 29-32.
[3] Liu, X.J. et al. (2001) On the analysis of a new spatial three-degrees-of-freedom parallel manipulator. IEEE Transactions on Robotics & Automation. Vol. 17, No.6: 959-968.
[4] Liu, X.J., Kim, J. (2002) A new three-degree-of-freedom parallel manipulator. Proc. IEEE International Conference on Robotics & Automation, Washington, DC: 1155-1160.
[5] Tsai, L.W., Joshi, S. (2001) Comparison study of architectures of four 3 degree-of-freedom translational parallel manipulators. Proc. IEEE International Conference on Robotics & Automation, Seoul, Korea: 1283-1288.
[6] Tsai, L.W., Joshi, S. (2002) A comparison study of two 3-DOF parallel manipulators: One with three and the other with four supporting legs. Proc. IEEE International Conference on Robotics & Automation, Washington, DC: 3690-3697.
[7] Company, O., Marquet, F., Pierrot, F. (2003) A New High-Speed 4-DOF Parallel Robot Synthesis and Modeling Issues. IEEE Transactions on Robotics and Automation, Vol.19, No.3: 411-420.
[8] Pierrot, F., Marquet, F. (2001) H4 parallel robot modeling design and preliminary experiments. International Conference on IEEE Robotics and Automation, Seoul Korea: 3256-3261.
[9] Li, C., Huang, Z. (2003) Type Synthesis of 5-DOF parallel Manipulator. Proc. IEEE International Conference on Robotics & Automation, Taipei, Taiwan: 1203-1208.
[10] M. H. Raibert and J. J. Craig (1981) Hybrid position and force control of robot manipulators, ASMS J. Dynamic System Measurement and Control, vol. 102: 126–133.
[11] R. Anderson and M. W. Spong (1987) Hybrid impedance control of robotic manipulators, Proc. IEEE International Conference on Robotics & Automation: 1073–1080.
[12] Chiaverini, S., Siciliano, B., Villani, L. (1998) Force and position tracking: parallel control with stiffness adaptation, Control Systems Magazine, Vol.18, Issue. 1, February: 27-33.
[13] Seul Jung, T. C. Hsia, and Robert G. Bonitz (2004) Force Tracking Impedance Control of Robot Manipulators Under Unknown Environment, IEEE Transactions on Control Systems Technology, Vol. 12, No. 3: 474-483.
[14] S. Jung, S. B. Yim, T. C. Hsia (2001) Experimental studies of neural network impedance force control for robot manipulators, Proc. IEEE Conference on Robotics & Automation: 3453–3458.
[15] S. Jung, T. C. Hsia (1998) Neural network impedance force control of robot manipulator, IEEE Transaction on. Ind. Electron., Vol.45, No.3: 451-461.
[16] K. Kiguchi, T. Fukuda (2000) Position/force control of robot manipulators for geometrically unknown objects using fuzzy neural networks, IEEE Transaction on. Ind. Electron., vol. 47: 641–649.
[17] S. Jung, T. C. Hsia (2000) Robust neural force control scheme under uncertainties in robot dynamics and unknown environment, IEEE Transaction on. Ind. Electron., vol. 47, No.2: 403–412.
[18] Morris, D. M., Hebbar, R., Newman, W. S. (2001) Force Guided Assemblies Using a Novel Parallel Manipulator, Proc. IEEE International Conference on Robotics & Automation, Seoul, Korea: 325-330.
[19] Gosselin, C. (1990) Stiffness Mapping for Parallel Manipulators, IEEE Transactions on Robotics and Automation, Vol.6, No.3: 377-382.